Phys. Med. Biol. **44** (1999) 1397–1417. Printed in the UK PII: S0031-9155(99)98219-2

Non-invasive measurement of chemotherapy drug concentrations in tissue: preliminary demonstrations of *in vivo* measurements

Judith R Mourant†, Tamara M Johnson†, Gerrit Los‡ and Irving J Bigio†

† Bioscience & Biotechnology Group, MS-E535, Los Alamos National Laboratory, Los Alamos, NM 87545, USA

‡ UCSD Cancer Center, La Jolla, CA 92117-0058, USA

Received 8 October 1998, in final form 17 December 1998

Abstract. Measurements of the tissue concentrations of two chemotherapy agents have been made *in vivo* on an animal tumour model. The method used is based on elastic-scattering spectroscopy (ESS) and utilizes a fibre-optic probe spectroscopic system. A broadband light source is used to acquire data over a broad range of wavelengths and, therefore, to facilitate the separation of absorptions from various chromophores. The results of the work include measurements of the time course of the drug concentrations as well as a comparison of the optical measurements with high-performance liquid chromatography (HPLC) analysis of the drug concentrations at the time of sacrifice. It is found that the optical measurements correlate linearly with HPLC measurements, but give lower absolute values.

1. Introduction and background

1.1. The need for non-invasive measurements and the goal of this work

The ability to non-invasively measure the concentrations of various drugs and compounds in tissues could provide a variety of benefits for pharmacological research and, ultimately, clinical applications. The advantages of non-invasive measurements for determining concentrations of chemotherapy and photodynamic therapy (PDT) drugs are numerous. Clinically, the therapeutic benefit of anticancer drugs is a function of the concentration–time profile in tumour tissue. It is important to know not only the time-course of the plasma concentration, but also the local tissue concentrations (Eichler and Muller 1998). Therefore, the ability to track the location and time-history of compound concentrations in tissue non-invasively would be advantageous for the development of new chemotherapy drugs (Kerr and Los 1993, Donelli *et al* 1992). The concentrations and kinetics of drugs at specific locations in the body are generally difficult to determine, given only the administered dosage or blood serum measurements. At present, however, there are very few minimally invasive or non-invasive methods for determining drug concentrations in tissue (Blochl-daum *et al* 1996).

The problem of determining *in vivo* tissue concentrations of various drugs is especially important for the development of PDT, a new treatment modality for cancer, wherein a site-selective drug is photoactivated with an appropriate wavelength of light. PDT (which is in various stages of FDA approval for several indications) is being investigated for treatment of

0031-9155/99/051397+21$19.50

several cancers including skin cancer, bladder cancer and carcinoma in the GI tract. (For recent reviews see Schuitmaker *et al* (1996), Dougherty *et al* (1998) and Chang and Bown (1997).) PDT is also being investigated for use in non-malignant diseases such as rheumatoid arthritis (Ratkay *et al* 1998) and the selective removal of endometrial tissue (Bhatta *et al* 1992, Fehr *et al* 1996). The ideal implementation of PDT requires delivery of the proper light 'dosage', which in turn requires understanding of the optical properties of the tissue and knowledge of the drug concentrations present in the tissue to be treated. *In vivo* measurements would provide information on patient–patient variability in the uptake of the drug and, therefore, make possible individual dosimetry for PDT. In addition, the site-specific time-history of the drug is especially important because the photoactivation should be done when the ratio of drug concentration in the tumour to surrounding tissue is at a maximum.

The method described here requires that the drug to be measured have a reasonably strong optical absorption band, somewhere in the range 330–1700 nm, but preferably not directly coincident with the strong bands of haemoglobin or water. Table 1 contains absorption peaks for several chemotherapy and PDT agents, demonstrating that there are a wide variety of compounds amenable to optical measurement. An important class of clinically approved anticancer agents are the anthracycline compounds and their analogues. Anthracyclines are pigmented and have indicator-like properties (red in acid and blue-violet in alkaline solution). Because of their pigmentation, anticancer agents that are anthracyclines (or analogues) are excellent candidates for non-invasive optical monitoring. This class of chemotherapy agents includes daunorubicin (= daunomycin), epirubicin and doxorubicin (= adriamycin), the last of which is examined in this paper. Derivatives of anthracyclines are still being developed (Choi *et al* 1998, Arcamone 1998). Another carbocyclic chemotherapy agent is mitoxantrone, which is also discussed in detail in this paper and which has strong absorption bands in the visible spectrum. Additionally, mitomycin C, an antitumour antibiotic, has strong absorption bands at 216, 360 and a weak band at 555 nm (Stevens *et al* 1965, Webb *et al* 1962). Taxol is available commercially in forms that are tagged with visible chromophores (Molecular Probes, Inc., Eugene, OR). All photodynamic therapy drugs (by design) have well-characterized visible/NIR absorption bands, in many cases due to porphyrins, with strong absorption coefficients, generally exceeding 10^4 M^{-1} cm^{-1} (Levy 1994). Because these absorptions are typically in the wavelength range of 600–800 nm, there is little interference from absorption by haemoglobin.

Table 1. Examples of important chemotherapy and PDT agents.

	Known bands (nm)	Observations
Chemotherapy agents		
Doxorubicin	479, 496, 529 (overlapping)	Broad band that lies between the main Hb bands
Mitoxantrone	608, 671	Very well suited
Mitomycin C	360, 555	
Taxol–tagged versions	500, 570	
PDT agents		All have well-suited red lines
Photofrin II (Haematoporphyrin derivative)	430, 630	
ALA/ protoporphyrin IX	430, 635	
Benzoporphyrin derivative	430, 690	
Zinc phthalocyanine	675	
mTHPC	420, 520, 652	

The primary goal of this work is to further develop a method and instrumentation for non-invasive, real-time measurement of changes in absorber concentrations (Mourant *et al* 1997a) and to apply this technique to *in vivo* measurements of chemotherapy agents in tissue. The method invokes a fibre-optic probe with a spectroscopic system, whose probe geometry can be compatible with clinical endoscopes, topical manipulation or small needles. A general schematic of the system components is shown in figure 1. In this paper we demonstrate the value of this method to pharmacology research by measuring the site-specific time-history of tissue drug concentrations in real laboratory research circumstances.

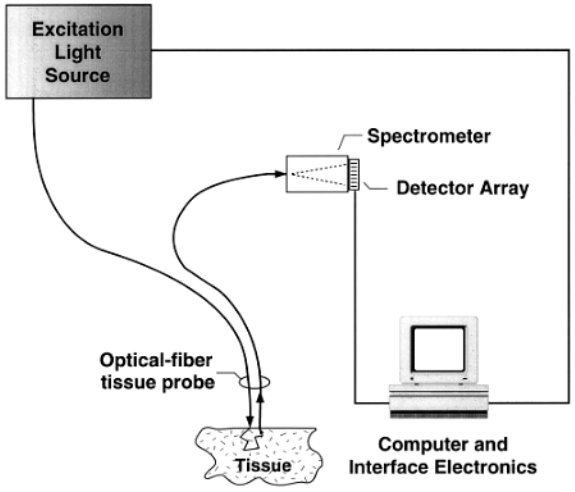

Figure 1. General component layout of the instrumentation.

1.2. Definitions of scattering and absorption parameters

In this paper we use the well-established optical parameters for describing scattering media, such as tissue: the scattering coefficient, $\mu_s(\lambda)$, is the inverse of the mean-free path between scattering events; the absorption coefficient, $\mu_a(\lambda)$, is the inverse of the absorption mean-free path; $P(\theta)$ is the probability of scattering through an angle θ and is also called the phase function; and the anisotropy factor, $g = \langle \cos\theta \rangle$, is the average cosine of the scattering angle. For most tissues the value of g is greater than 0.85 (Wilson 1995, Cheong *et al* 1990). It is also convenient to use the 'reduced scattering coefficient', which can be regarded as the inverse of an effective distance between direction-randomizing scattering events, and is defined as $\mu_s' = \mu_s(1 - g)$.

1.3. Current invasive methods for in situ measurement

Generally a biopsy or surgical tissue extraction must be performed in order to assay drug concentration in tissue. This very invasive technique makes measuring time-histories difficult. With small-animal studies, numerous animals are often sacrificed at different time intervals after administration of the drug, permitting the tissue to be taken from target organ sites for assay.

Less invasive than surgical biopsy is the method of microdialysis, which invokes small, implanted, needle-shaped probes (Rossomondo and Kehr 1998). Microdialysis is a technique

for sampling the extracellular fluid and is typically combined with HPLC to determine the concentration of analytes in the extracellular fluid. Microdialysis probes have proved to be useful for *in vivo* measurement of local tissue concentrations of low molecular weight compounds in extracellular fluids. There are, however, difficulties in implementing this technology and it has limitations (Humpel *et al* 1996). Some difficulties arise from the fact that microdialysis probes are inherently invasive. The area around the probe can become inflamed (Davies and Lunte 1995) and damage to the tissue may alter the biochemistry of the tissue (Humpel *et al* 1994, Layton *et al* 1997). Another limitation of microdialysis is that the probes only extract compounds from extracellular fluid; no information is obtained about concentrations in the cells themselves or in the capillary bed. Chemotherapy agents often intercalate in DNA or bind to proteins and other components of the cells. Therefore, information about the intracellular concentrations can be important.

1.4. Optical approaches to non-invasive measurement

There has been very little published on optical measurement of tissue concentrations of chemotherapy agents. However, several groups have reported that measurement of PDT-drug fluorescence can provide important information for dosimetry (Star 1997, Rhodes *et al* 1997, Braichotte *et al* 1996). Some chemotherapy agents, and some of the PDT drugs, however, are not fluorescent, and therefore cannot be measured by fluorescence techniques. Therefore, absorption measurements are more general techniques. Furthermore, the light intensity to be measured is larger (and therefore less expensive equipment is needed), and photobleaching is not an issue.

For modest intensities, the predominant responses of tissue to light are scattering and absorption. Both exhibit variations with wavelength in ways that reflect various parameters of the tissue structure and biochemistry. The absorption and reduced scattering coefficients may be determined from photon transport when measurement geometries are such that diffusion theory is applicable. This may be done with time-resolved, frequency-domain or steady-state measurements. The applicability of the time-resolved technique for measuring the tissue concentration of a PDT drug has been demonstrated (Patterson *et al* 1990). The time-domain and frequency-domain methods both employ relatively complex instrumentation, making clinical application difficult and/or costly. The use of narrow-bandwidth light sources in these techniques limits the use of these methods to measuring compounds that have absorption bands at the specific wavelengths of the light sources (and which do not overlap intrinsic absorption bands). A combination of several light sources can allow for broader wavelength measurements (Fantini *et al* 1994), but further increases the cost of instrumentation.

Broad-wavelength, steady-state measurements based on diffusion theory have also been investigated as a method for measuring absorption coefficients (Farrell and Patterson 1992, Nichols *et al* 1997, Mourant *et al* 1997b, Lin *et al* 1997) and photosensitizer concentrations have been measured *in vivo* using this method (Weersink *et al* 1997). For measurement of the concentration of phthalocyanine tetrasulfonate in skin, the non-invasive estimate was found to be proportional to the true concentration, but lower by a factor of three. In the case of liver tissue, better agreement was found. The inaccuracies of the measurement of skin are probably related to the fact that the tissue measured was quite inhomogeneous.

In all diffusion theory-based methods, the separations between light delivery and light collection are of the order of millimetres to centimetres, and the volume probed is of the order of 1 cm^3. The large separation of the source and detector results in large distances of photon travel and therefore a strong sensitivity to absorption. On the other hand, because of strong absorption by haemoglobin bands and detector limitations, large-distance measurements are

limited to a spectral range of about 600–950 nm, reducing the number of drugs that can be monitored. Additionally, the spatial resolution is low due to the large tissue volume that is probed.

1.5. Elastic-scattering spectroscopy

Elastic-scattering spectroscopy (ESS) refers to broadband white-light measurements made in the optical geometry shown in figure 2, wherein separate illuminating and collecting fibres are placed in direct optical contact with the tissue. With this method, surface reflections are avoided and all of the collected light has undergone multiple scattering through the tissue in making its way from the illuminating fibre to the collecting fibre. Optical signatures of tissue, based on ESS, can be used to non-invasively diagnose malignancy and other tissue pathologies in certain organs (Mourant *et al* 1995, 1996a, Perelman *et al* 1998, Ge *et al* 1998).

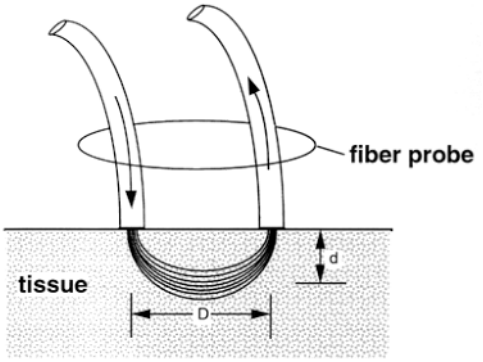

Figure 2. Depiction of the typical optical geometry used for elastic-scattering spectroscopy.

Elastic-scattering spectroscopy can be used to measure absorption coefficients in much smaller volumes than the diffusion theory-based methods described in section 1.4. Methods for measuring bilirubin concentrations are being developed based on an iterative algorithm, which takes prior measurements of the reduced scattering coefficient as input (Jacques *et al* 1997). Both that work and the work described here make use of Beer's law. When the pathlength of photon travel is known, Beer's law can be used to determine the absorption coefficient. (This is described in detail in sections 1.6 and 3.1–3.4.) The pathlength of photon travel in a scattering medium generally depends on the scattering parameters of the medium. In a previous publication (Mourant *et al* 1997a) we demonstrated that for an appropriate range of fibre separations, ρ, between light delivery and collection fibres, the pathlength of the collected photons, L, is insensitive to variations in scattering parameters for the range of scattering parameters typically found in tissue. For the range of tissue scattering parameters encompassed by the values $\mu_s' = 5$–$15\ \mathrm{cm}^{-1}$, L is least sensitive to variations in μ_s' when ρ is in the range 1.5–2.2 mm. If there is significant absorption, this range broadens to 1.5–2.6 mm.

The idea of a 'special' fibre separation can be motivated by an intuitive examination of how scattering affects the pathlengths for very small and for very large source–detector separations, in the optical geometry of figure 2. In general, for very small fibre separations, the distance travelled by the collected photons is longer for a less-scattering medium with higher values of g than for a highly scattering medium and lower values of g, because the photons need to do a quick 'U-turn' (undergoing a certain number of high-angle scattering events) in order to nearly reverse their direction of travel and reach the adjacent collection fibre. On the other hand,

for large fibre separations photon scattering becomes isotropic (the photons 'forget' about the orientation of the illumination fibre) and the distance travelled is simply longer for higher scattering coefficients because more collisions are made between entrance and exit. (The case of large separation becomes similar to the conceptually simpler case of light transport from one side to the other of a scattering slab.) Therefore, there must be some cross-over regime of intermediate values of fibre separation, for which the distances travelled by collected photons are relatively insensitive to changes in scattering parameters.

In a highly scattering medium, there is a distribution of photon paths. Since, this work focuses on measuring absorption coefficients, we are interested in the 'effective' pathlength only as it is related to Beer's law. As discussed in an earlier paper (Mourant *et al* 1997a), the 'effective' pathlength, L, in which we are interested is not the same as the average of the pathlengths travelled by the collected photons. A method for experimentally determining L is described in section 3.2.

Recently, it was reported that the optimal fibre separation for minimizing the sensitivity of the collected surface fluence to variations in the reduced scattering coefficient is about 3.3 mm (Schmitt and Kumar 1997). An important point is that this surface fluence is a different parameter from the photon pathlength, L, which was shown to be insensitive to scattering changes for a $\sim$1.7 mm source–detector separation (Mourant *et al* 1997a). Therefore, it is not surprising that different optimal fibre separations were obtained when minimizing sensitivity to two different parameters. Since L is the parameter of concern when using Beer's law to determine absolute concentrations of an absorber, we chose 1.7 mm as the optimal fibre separation for this work.

When compared with measurement at discrete (or a narrow range of) wavelengths, a broadband measurement enables generation of the complete spectral shape of the absorption, including both the drug of interest and the native absorption bands. This broad spectral measurement permits accounting for (and quantifying) contributions by native chromophores; it may provide information relevant to the local environment of the drug, and could be useful in determining the presence of metabolites. Tracking changes in native chromophores such as haemoglobin and oxy-haemoglobin can be helpful in evaluating the response of a tumour to the therapy.

1.6. General theory of the measurements

The basic approach taken in this work is to measure the elastic scatter signal before administration of a drug (time t_0) and then at several times after administration of the drug. These measurements are then used to determine the change in absorption of the tissue due to the presence of the drug, between time t_0 and a later time t. Beer's law which requires knowledge of L is used as the basis for the analysis. Equation (1) is Beer's law, where $I(t)$ is the collected light at time t, $\Delta\mu_a$ is the change in the absorption coefficient of the medium (from t_0 to t), and $I(t_0)$ is the collected light at time t_0:

$$I(t) = I(t_0)\exp(-\Delta\mu_a L). \tag{1}$$

(Geometric factors, such as numerical aperture, and system response are assumed to be constant between t and t_0.) A time-dependent change in absorption may then be expressed as

$$\mu_a(t) - \mu_a(t_0) = -\ln\left(\frac{I(t)}{I(t_0)}\right)L^{-1} \tag{2}$$

where t_0 represents the time just prior to the addition of the absorber. Modifications of equation (2) will be required to accommodate time-dependent changes in scattering properties.

As will be presented in sections 3.1 and 3.2, two sets of correction terms must be applied to equation (2) in order to accommodate the complexities of *in vivo* measurements. The chosen fibre separation ensures that L does not change with scattering properties, but it does not ensure that the amount of collected light will not change. The relevant modification of equation (2) is addressed in section 3.1. Additionally, equation (2) is strictly valid only over a range of wavelengths for which there are no large changes in absorption, which would cause a wavelength dependence of L. A method for dealing with this second complication is described in section 3.2.

2. Materials and methods

2.1. Instrumentation

A schematic diagram of the instrumentation is shown in figure 1. The illumination light source was a pulsed xenon short-arc lamp, driven as a pulse burst during the 50 ms integration time of the detector. (The total light incident on the tissue was less than 1 mJ.) Light was delivered to the tissue and collected from the tissue using optical fibres (as shown schematically in figure 2). The delivery fibre was 400 μm in diameter and the collection fibre was 200 μm in diameter. Both fibres had a numerical aperture of 0.22. The centre-to-centre separation of the fibres was 1.7 mm, for the reasons discussed in section 1.5. An SD2000 miniature spectrometer (Ocean Optics, Inc.) was used in the *in vivo* studies for dispersion and detection of the collected light. Nonlinearity in the response of the detector was corrected for in the data analysis. The tissue phantom studies were performed with an Acton 275i spectrograph (Acton Research Corp.) for dispersion of the collected light and a TE-cooled CCD (Princeton Instruments, Inc.) for detection of the light. To account for the wavelength dependence of the light source, fibres, and light detection system, a reference measurement of reflectance from a spectrally flat diffuse reflector was made (Spectralon, Lab Sphere Inc.).

2.2. Phantom studies

A suspension of Intralipid (a fat emulsion), with $\mu_s' \sim 7$ cm^{-1} at 550 nm, was used to provide a scattering phantom and Direct Blue Dye #71 (ACS #4399-55-7) was used as an absorber. An elastic-scatter spectrum of the Intralipid suspension was taken before any dye was added and then after each addition of blue dye. Sixteen aliquots of blue dye were added. After the addition of the sixth and the eleventh aliquots of dye, the scattering properties of the solution were changed by adding a small amount of concentrated Intralipid. The first produced a change of 17.4% in μ_s', and after the final change, the reduced scattering coefficient had increased by 34%.

A suspension of polystyrene spheres (diameter $\sim$0.895 μm) was used to provide a second tissue phantom with $\mu_s' \sim 14$ cm^{-1} at 550 nm. The blue dye was again used to alter the absorption properties of this phantom. An independent absorption spectrum of this dye in a non-scattering aqueous solution was measured on a Cary spectrophotometer to determine the absorption coefficient of the stock solution of the dye.

2.3. Induction of tumours in mice and administration of chemotherapy drugs

Four Nu/Nu ('Nude') mice (20 g) were inoculated subcutaneously with human squamous-cell carcinoma cells (2×10^6) at four sites: left and right shoulders and left and right hips. Four weeks later subcutaneous tumours were present in all mice. The tumour size ranged from 0.5 to 1 cm in diameter. Three of the mice were treated with doxorubicin and one with mitoxantrone,

by injection into the peritoneal cavity. Elastic-scattering spectroscopy measurements for each mouse were performed through the skin on each tumour location, on the right thigh muscle, and on the peritoneal cavity. These measurements were made prior to administration of the drug, and at a series of times following administration, up to the time of sacrifice.

The administered dosages, and the times of sacrifice were:

- Doxorubicin: 4 mg kg^{-1} (a typical therapeutic dose): sacrificed at 22 h (mouse 1)
  16 mg kg^{-1} (a larger than normal dose): sacrificed at 7.5 h (mouse 2)
  16 mg kg^{-1} (a larger than normal dose): sacrificed at 4 h (mouse 4).
- Mitoxantrone: 1 mouse at 3 mg kg^{-1} (a typical therapeutic dose): sacrificed at 7.5 h (mouse 3).

Following sacrifice the tumours and the appropriate thigh muscles were harvested. Some optical measurements were made directly on a few of the extracted tumours. For the mice treated with doxorubicin, the tissues were processed, and HPLC assays were performed to determine the drug concentrations in the tumours/muscles at time of sacrifice. This permitted direct comparison of the final absolute concentration measured optically with an independent assay method. Doxorubicin was extracted from the tissues using a chloroform:isopropanol (1:1) extraction method. (Recoveries of doxorubicin were 85 to 90%.) Doxorubicin concentrations were determined by HPLC using a fluorescence monitor (excitation 470 nm, emission 550 nm) and epirubicin as the internal standard. The mobile phase consisted of acetonitrile: 0.035 M HCOOH-$HCOONH_4$ buffer, pH 4.2 (35:65). No HPLC data were available for mitoxantrone.

2.4. Optical measurements of tumours and muscles

The optical measurements were made by touching the tip of the fibre probe at right angles to the skin surface and triggering the system. The system measures the 'dark' background and then fires the light source for the 50 ms pulse burst. The 'dark' measurement is subtracted from the measurement with the lamp. The tissues were measured before administration of the chemotherapy agents and at several times after administration. All of the measurements that were made prior to sacrifice were done across the thin skin over each site, to preserve the intended non-invasive character of the measurements. This method was assumed to be reasonable since the skin over the tumours was stretched thin ($\sim$200 μm) and constituted a small fraction of the total pathlength of the collected photons.

2.5. Spectra of haemoglobin, doxorubicin and mitoxantrone

Absorption spectra of aqueous solutions of doxorubicin and mitoxantrone, as well as oxy- and deoxy- bovine haemoglobin, were measured with spectrophotometers. Deoxyhaemoglobin was obtained by reducing bovine haemoglobin (Sigma Chemical Co) with sodium dithionite in an argon atmosphere. Oxyhaemoglobin was obtained by adding oxygen to the deoxyhaemoglobin sample. The measured haemoglobin spectra agreed well with literature values (Zijlstra 1991) below 600 nm, but not at longer wavelengths. Therefore, below 600 nm we used our measured values (which were taken at much higher resolution) and above 600 nm we used data taken from Zijlstra (1991). The spectrum of doxorubicin depends strongly on solution conditions. Rather than using our measured spectra we chose to use a spectrum of the DNA-bound form (Porumb 1978), which is likely to be more relevant for the *in vivo* conditions. The spectra used for data analysis are shown in figure 3.

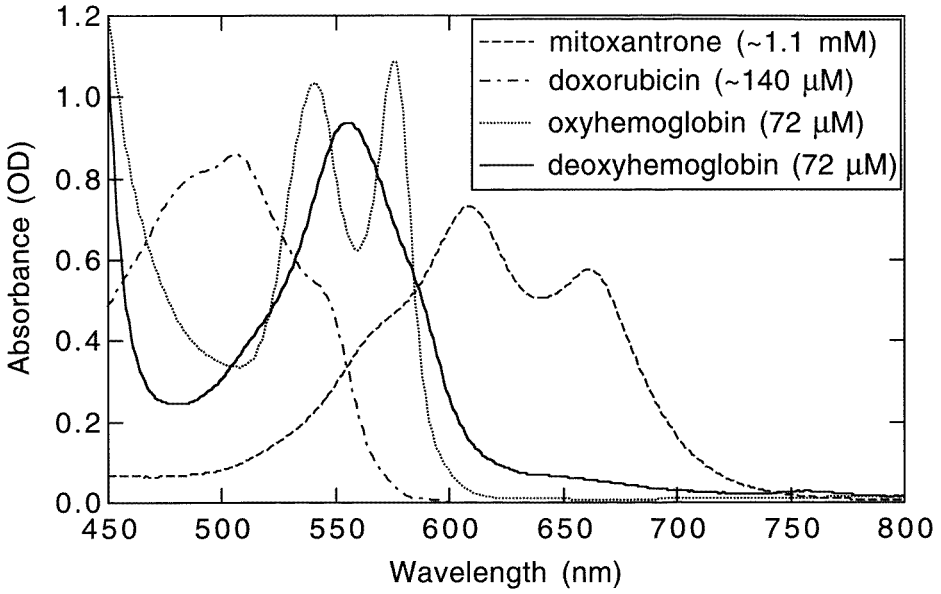

Figure 3. Spectra of oxyhaemoglobin, deoxyhaemoglobin, doxorubicin and mitoxantrone. The spectrum of doxorubicin is of the DNA-bound form and was taken from Porumb (1978).

2.6. Data fitting

For all fitting of experimental spectral data to theoretical curves discussed in the results section, a Levenberg–Marquardt algorithm was used to search for coefficient values and minimize chi-squared.

2.7. Monte Carlo simulations

In the Monte Carlo simulations photons are propagated in a manner similar to that described by Wang and Jacques (Jacques and Wang 1995, Wang *et al* 1995). The distance between scattering events was determined based on the value of μ_s and the probability of absorption for a given distance travelled was calculated using μ_a. As the photons were propagated, the positions of scattering events were recorded for the collected photons. The average distance travelled by the collected photons in going from the source fibre to the detection fibre was also computed. Methods for the initial launch of the photons and for their termination have been described earlier (Mourant *et al* 1996b). For this work the angular probability distribution for scattering, i.e. the scattering phase function, which was employed was the well-known Henyey–Greenstein approximation (Henyey and Greenstein 1941).

3. Results

3.1. Changes in scattering properties between measurements do not affect absorption measurements

As discussed in section 1.5, we have shown in previous work that with the proper choice of fibre separation, the pathlength travelled by the photons is relatively insensitive to variations

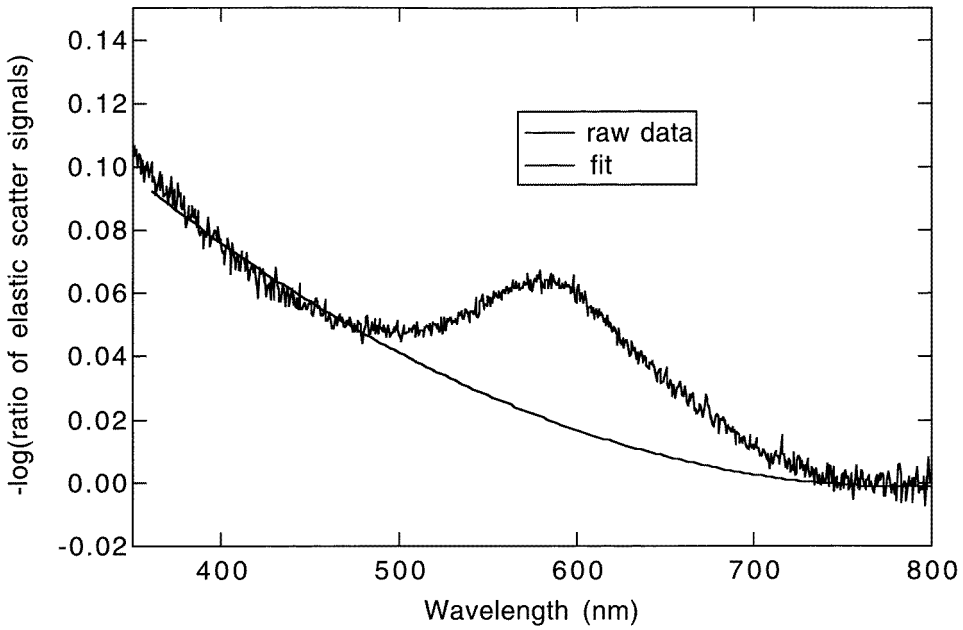

Figure 4. Raw data from measurements of blue dye in an Intralipid suspension and the fit used for baseline correction.

in scattering parameters (Mourant *et al* 1997a). It was demonstrated that analysis of measurements of a scattering medium made before and after addition of an absorber yielded the same value of absorption coefficient regardless of the scattering properties of the medium. However, in that work, changes in scattering properties between (elastic-scatter) measurements for a given location as a function of time were not considered. This type of situation is likely to occur in tissue, either because of a change in physiological scattering properties or because of slightly different placement of the probe at different times. It should be repeated here that although L is insensitive to scattering changes for the chosen fibre separation, the amount of collected light is sensitive to scattering changes.

To address this issue measurements were made on an Intralipid-based tissue phantom, and the scattering properties were changed between some of the measurements of the elastic-scatter signal. Spectral measurements of the tissue phantom were analysed by taking the ratio of a given spectrum after addition of blue dye to the spectrum taken before any dye was added. The negative log of each resulting spectral ratio was then computed. An example of the resultant spectra is shown in figure 4. The absorbance of the blue dye is clearly present, but there is also a slowly varying baseline in this example. This baseline is due to the fact that the scattering parameters changed between the two measurements of the elastic-scatter signal, and therefore the wavelength dependence of the collected light changed, although L did not. To account for this baseline shift, the data outside of the region of absorbance of the dye were fitted to the expression

$$c_0 + c_1\lambda + c_2\lambda^2$$

where c_0, c_1 and c_2 are coefficients that are varied in the fit, and λ is the wavelength. The baseline term was then subtracted from the spectral data at all wavelengths and the concentration of blue dye determined from the peak height of the corrected spectral band. In this experiment

there were two occasions at which the scattering parameters were changed. The absorbances calculated before and after the change in scattering properties were less than 8% different from each other in both cases.

3.2. Accounting for the dependence of pathlength on μ_a.

The other required modification of equation (2) is accounting for the variation in L with the total absorption coefficient. Although L is insensitive to variations in scattering properties for the chosen source–detector separation, it does depend on absorption. The more absorbing a medium is, the shorter L is. This is important for *in vivo* measurements, where there may be strong absorption due to haemoglobin, which affects the pathlength of collected photons.

To examine how absorption affects L, Monte Carlo simulations were run with a variety of absorption coefficients, and the pathlengths were calculated. It was found that equation (3) can describe the dependence of pathlength on absorption:

$$L(\mu_a) = x_0 + x_1 \exp(-x_2\mu_a). \tag{3}$$

The values of the coefficients x_0, x_1 and x_2 in equation (3), were determined from measurements in a phantom. Specifically, ESS measurements were made in a suspension of polystyrene spheres before and after the addition of each of 20 aliquots of blue dye. The ESS measurements were analysed by taking the ratio of a given spectrum after each addition of dye to the spectrum taken before any dye was added. The negative log of each resulting spectral ratio was then computed. These spectra were then fitted to equation (4)

$$\begin{aligned} -\log(I(t)/I(t_0)) &= c_0(t) + c_1(t)\lambda + c_2(t)\lambda^2 \\ &+[C_{\text{dye}}(t)\varepsilon_{\text{dye}}(\lambda)][x_0 + x_1 \exp(-x_2 C_{\text{dye}}(t)\varepsilon_{\text{dye}}(\lambda))] \end{aligned} \tag{4}$$

where C_{dye} is the concentration of blue dye and $\varepsilon_{\text{dye}}(\lambda)$ is the measured extinction coefficient of a non-scattering aqueous solution of the dye. The parameters that were allowed to vary during the fits were c_0, c_1, c_2 and the concentration of blue dye, C_{dye}. The values of the parameters x_i were fixed for a given set of fits. The values of x_i were established by performing several sets of fits with different values of x_i until agreement between experimental and known values of the concentration of blue dye were obtained. Results of the measurements are shown in figure 5.

3.3. Absorption spectra of chemotherapy drugs

Absorption spectra of the two chemotherapy drugs used in this study, doxorubicin and mitoxantrone, are shown in figure 3. Mitoxantrone has peaks near 610 and 661 nm as expected from the literature (Feofanov *et al* 1997, Mewes *et al* 1993). The absorption spectrum of doxorubicin was taken from Porumb (1978) and is the DNA-bound form. It is characterized by a blending of bands, resulting in a broad absorption feature from 440 to 540 nm (FWHM), due to the presence of the dihydroxyanthraquinone chromophore (Porumb 1978, DiMarco *et al* 1969).

3.4. Results of in vivo measurements on mice

Based on the results of sections 3.1 and 3.2, equation (5) is a general equation, which was used in analysing the *in vivo* measurements on mice. The elastic-scatter spectra measured before and after a change in absorbance are I_1 and I_2 respectively. The baseline term, B, is quadratic

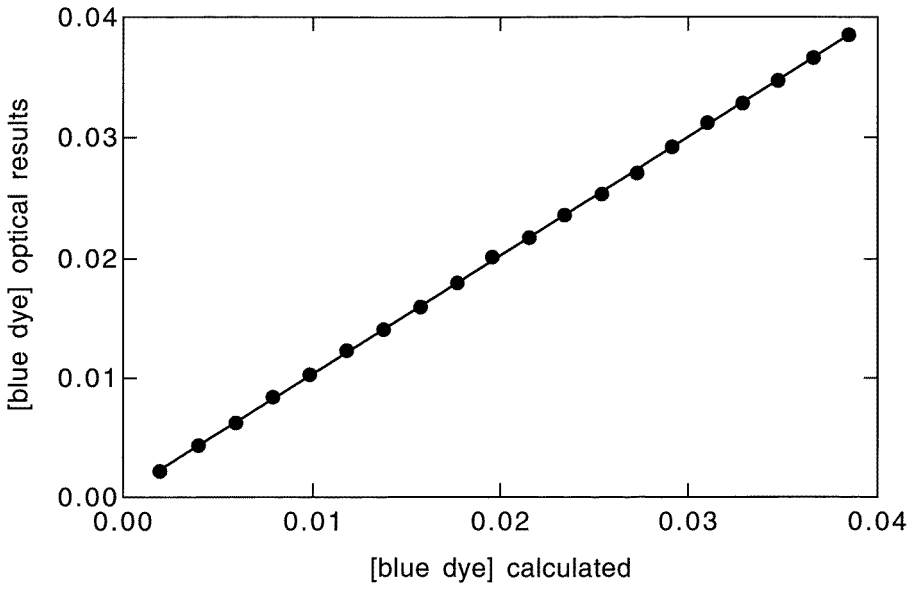

Figure 5. The correlation between the optical measurement of concentration of a blue dye added to a suspension of polystyrene spheres and the calculated concentration of blue dye. The units are in amounts of a stock solution present and are the same for both axes.

in wavelength and c_0, c_1 and c_2 are fitting parameters. The pathlength function (i.e. $L(\mu_a)$) is given by equation (3) with x_i set to be the experimentally determined values: $x_0 = 0.6$ cm, $x_1 = 1.3$ cm and $x_2 = 3.565$ cm.

$$-\log(I_2/I_1) = B + \Delta\mu_a L(\mu_a) \tag{5}$$

where

$$B = c_0 + c_1\lambda + c_2\lambda^2 \quad \text{and} \quad L(\mu_a) = x_0 + x_1 \exp(-x_2\mu_a).$$

The last term on the right-hand side of equation (5) is a function of the total absorption. Therefore, in order to analyse the data it is necessary to have a measure of the total absorption. Since it is impossible to make measurements in the absence of haemoglobin, the elastic-scatter spectrum in the absence of haemoglobin was approximated. This approximation was done by fitting a straight line to the wavelength range from 750 nm to 800 nm of the initial elastic scatter measurement for each specific location and extrapolating this line over the entire wavelength range of interest. (The wavelength range 750–800 nm was used because the intrinsic absorption in tissue is very small in this region.) Equation (5) could then be used to determine the amount of haemoglobin present at the start of the measurements ($C_{\mathrm{HbO}}(t_0) + C_{\mathrm{Hbd}}(t_0)$), where I_1 is the straight-line extrapolation, I_2 is the initial elastic scatter measurement of a specific location, and $\mu_a = \Delta\mu_a$ are given by

$$\mu_a = \Delta\mu_a = C_{\mathrm{HbO}}(t_0)\varepsilon_{\mathrm{HbO}}(\lambda) + C_{\mathrm{Hbd}}(t_0)\varepsilon_{\mathrm{Hbd}}(\lambda). \tag{6}$$

C_{HbO} and C_{Hbd} are the concentrations of oxygenated and deoxygenated haemoglobin respectively, and $\varepsilon_{\mathrm{HbO}}(\lambda)$ and $\varepsilon_{\mathrm{Hbd}}(\lambda)$ are the measured extinction coefficients of oxygenated and deoxygenated haemoglobin respectively.

Once the initial haemoglobin concentrations were determined, the elastic-scatter measurements at times after administration of the drug were used to measure the time course

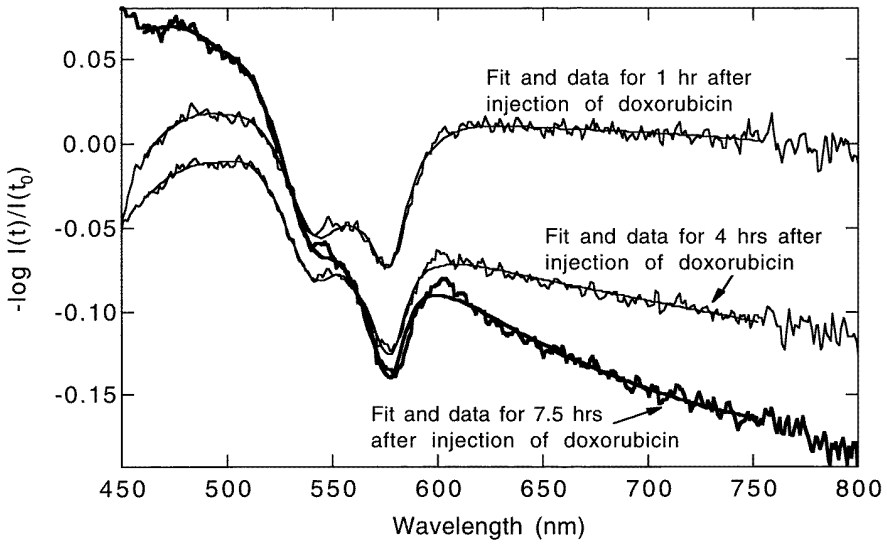

Figure 6. Fits to the spectra obtained *in vivo* from a mouse injected with doxorubicin.

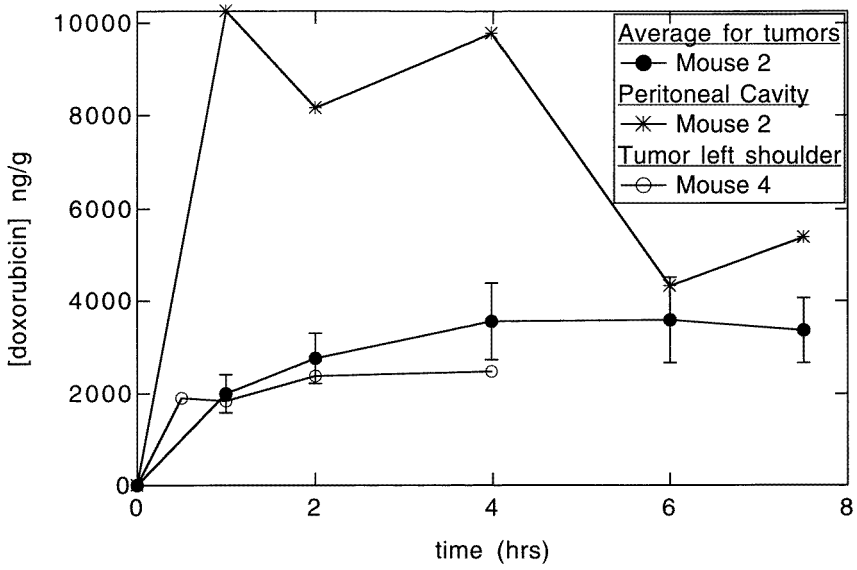

Figure 7. Concentration of doxorubicin as a function of time as calculated from the optical measurements. The concentration in the peritoneal cavity and an average of the concentration in the four tumours is shown for mouse 2. The concentration in the tumour in the left shoulder is also shown as a function of time. The units on the y-axis are nanograms of doxorubicin per gram of tissue. It was assumed that the density of tissue was 1.0 gm cm^{-3}. The error bars shown for the tumour averages of mouse 2 are a calculated standard deviation of the measurements on the four tumours. They are therefore representative of a combination of the error in the measurements and the variation in the amount of doxorubicin present in the different tumours.

of the drug concentration in the tissue. This analysis was done using equation (5), with I_2 being the spectrum measured at time t, I_1 being the initial spectrum measured at time t_0, and

μ_a and $\Delta\mu_a$ given by equations (7*a*) and (7*b*) respectively:

$$\Delta\mu_a = \Delta C_{\mathrm{HbO}}(t)\varepsilon_{\mathrm{HbO}}(\lambda) + \Delta C_{\mathrm{Hbd}}(t)\varepsilon_{\mathrm{Hbd}}(\lambda) + C_{\mathrm{drug}}(t)\varepsilon_{\mathrm{drug}}(\lambda) \quad (7a)$$

$$\mu_a = \{\Delta C_{\mathrm{HbO}}(t) + C_{\mathrm{HbO}}(t_0)\}\varepsilon_{\mathrm{HbO}}(\lambda) + \{\Delta C_{\mathrm{Hbd}}(t) + C_{\mathrm{Hbd}}(t_0)\}\varepsilon_{\mathrm{Hbd}}(\lambda) + C_{\mathrm{drug}}(t)\varepsilon_{\mathrm{drug}}(\lambda). \quad (7b)$$

For doxorubicin, the fits were performed over the wavelength range 460 to 700 nm.

Example results of these fits are shown in figure 6. Figure 7 shows the time-history of the measured drug concentrations for two of the mice, which were injected with 16 mg kg^{-1} doxorubicin and sacrificed at 4 and 7.5 h. Results are given for the average drug concentration in the four tumours of mouse 2 and for one tumour of mouse 4. The drug concentration in the peritoneal cavity (divided by 5) is also given for mouse 4. As expected, the concentration of drug in the peritoneal cavity decreases with time (following the initial injection), while the concentration in the tumours initially increases with time.

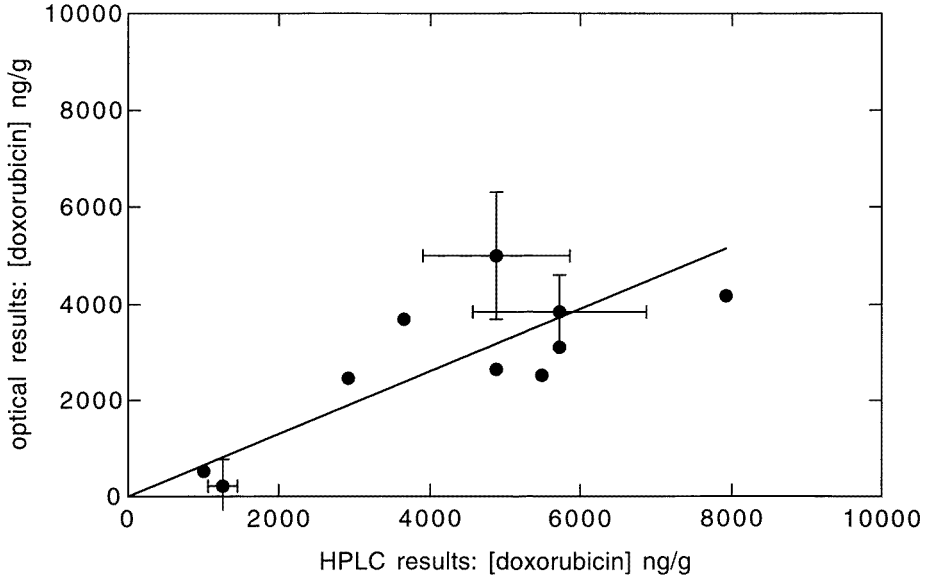

Figure 8. Comparison of the amount of doxorubicin present at the time of sacrifice as measured by *in vivo* optical measurements and after tumour removal by HPLC. For clarity, error bars are only shown where multiple optical measurements were made on the same tumour and the standard deviation could be computed. The error bars for HPLC are 20% of the measured value.

Figure 8 shows the correlation between measurements of concentration performed by ESS immediately before sacrifice compared with the corresponding HPLC results for the three mice treated with doxorubicin. The two data points corresponding to the lowest doxorubicin concentrations are from mouse 1. The mouse 1 point without error bars is the average of the results for the four tumours. The point with error bars is the average of five optical measurements on one tumour after harvest. All other data points are from mice 2 and 4. Those without error bars are single optical measurements. Those with error bars are the average of five optical measurements on a single tumour after harvest. (Measurements of two tumours on mouse 4 were not used, because strong haemoglobin absorption caused these spectra to be unusually noisy.) A straight line fit to the data points in figure 8 which was forced to go through 0,0 is also shown in figure 8. The slope of this line is 0.65 ± 0.08. Ideally, the slope of this line would be 1.

Analysis of ESS spectra for the mouse injected with mitoxantrone was greatly simplified due to the fact that mitoxantrone has absorbance peaks that are separated from the haemoglobin bands. These data were fitted to equation (5), with $\mu_a = \Delta\mu_a$ given by equation (8) over the wavelength range 614–750 nm.

$$\mu_a = \Delta\mu_a = C_{\text{mito}}(t)\varepsilon_{\text{mito}}(\lambda). \tag{8}$$

In this case the baseline-term is being used to account not only for the slow wavelength-dependent scattering effects, but also for the changes in the small haemoglobin absorption in this wavelength range. Examples of fits are shown in figure 9. Fits were performed both with the measured mitoxantrone spectrum and a spectrum shifted by 18 nm to simulate a DNA bound mitoxantrone spectrum (Feofanov *et al* 1997).

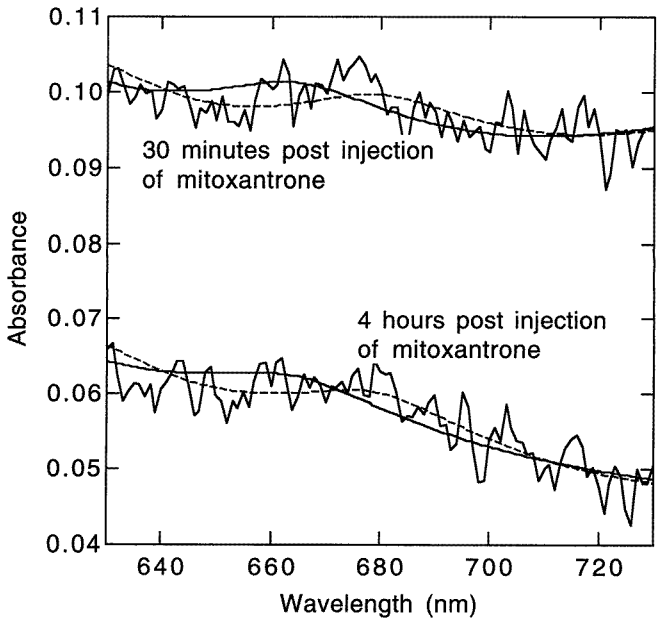

Figure 9. Examples of fits to spectra measured *in vivo* to obtain the amount of mitoxantrone present. The full curves are the fits performed using the mitoxantrone spectrum shown in figure 3. The broken curves are fits performed using a mitoxantrone spectrum shifted by 18 nm to approximate the DNA-bound form.

The time courses for two tumours and the right thigh muscle are shown in figure 10. It appears that very little drug was taken up by the tumour in the right hip, and that much more drug is taken up by the right thigh muscle than by either of the tumours. For all tumours, the amount of drug in the tumours increases over a period of at least 4 h.

4. Discussion

4.1. Possible interferences and sources of error

The optical absorption by chemotherapy drugs at therapeutic doses in tissue is expected to be smaller than that of haemoglobin for wavelengths shorter than 610 nm. Therefore, measurement of drugs with spectral absorption bands overlapping the α, β and Soret bands of

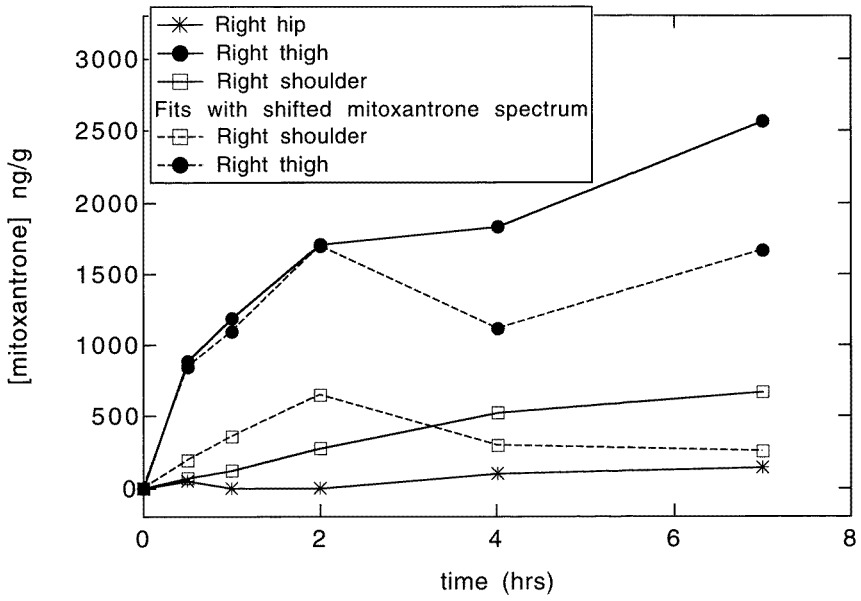

Figure 10. Concentrations of mitoxantrone in the right thigh and tumours in the right hip and right shoulder as a function of time after injection of the drug.

haemoglobin is difficult. Accurate spectra of both the measured drug and of haemoglobin are needed. It is possible that the bovine haemoglobin spectra used in analysing the data in this paper do not accurately represent the absorption of blood in these mice, and this may be one source of error in the fits. A further source of error may be smaller endogenous absorptions, which were not taken into account in our analysis. For example, in several of the fits a significant discrepancy was found between the data and the fits at about 605 nm. Furthermore, strong evidence for the presence of another absorber in the peritoneal cavity was found, as several spectra from this location (although not for any of the tumours) showed an absorption peak at about 670 nm.

The spectra of both doxorubicin and mitoxantrone are affected by their environment. In the case of mitoxantrone, the relative ratio of the absorption maxima (near 615 and 665 nm) depends on the amount of the monomeric and dimeric forms present, which is controlled by solution conditions. Mitoxantrone is also known to bind to micelles and DNA. Interactions with micelles do not affect the absorption spectra. Intercalation with DNA, however, causes a significant red-shift of the absorption peaks. The two absorption bands shift from 610 nm to 628 nm and from 661 nm to 680 nm respectively (Feofanov *et al* 1997). There are also several metabolites of mitoxantrone—some with red-shifted absorption spectra and some with blue-shifted absorption spectra (Mewes *et al* 1993).

In analysing the *in vivo* mitoxantrone data it was found that the peak absorption of mitoxantrone at about 660 nm was shifted to the red. In the peritoneal cavity (where the optical absorption of the drug is greatest and this spectral shift is easily measured) a strong absorption with a maximum at 681 ± 3 nm was present. This is consistent with mitoxantrone being present primarily in a nucleic acid-bound form. It is unlikely that this spectral shift is caused by the presence of metabolites, since the conversion of mitoxantrone to its metabolites is only about 20% complete after 8 h in rat hepatocytes, and some of the metabolites have blue-shifted absorption spectra (Mewes *et al* 1993). The mitoxantrone data were analysed

with both the original spectrum and an 18 nm shifted spectrum. There was no significant difference in chi-squared for the right shoulder, right hip, left shoulder or left hip between fits with the two different mitoxantrone spectra. However, chi-squared was lower for the right thigh and peritoneal cavity data when the shifted mitoxantrone spectrum was used.

The spectrum of doxorubicin is sensitive to its environment and is also modified upon binding to DNA (Porumb 1978). The choice to use the DNA-bound spectrum in this work was somewhat arbitrary, although motivated by the fact that the mitoxantrone spectra showed evidence of being present in the DNA-bound form. Data analysis was also performed based on an aqueous solution spectrum of doxorubicin. The results were qualitatively similar to those obtained with the DNA-bound spectrum, i.e. there was a correlation between the HPLC and optical results, but the absolute values of the optical results differed from those obtained by HPLC.

The photon pathlengths for the initial measurements at time t_0 may be slightly different from the pathlengths for the measurement at time t. Our analysis assumes that these pathlengths are the same and a difference in them would cause an error in the determination of μ_a. For the determination of chemotherapy drug concentrations this error should be small, because the changes in absorption (due to addition of the drug and changes in haemoglobin concentration and oxidation) between the measurements at times t_0 and t are relatively small and therefore cause only a minor perturbation in L. (There is probably a larger error in the calculation of the amount of haemoglobin initially present. This error, however, will only have a small effect on calculations of drug concentration through the consequent error in L for those calculations.) We have chosen to use the pathlength that is appropriate for the measurements at time t. In our analysis of blue dye in a suspension of spheres, this method of analysis gave excellent results.

Some of the spectra obtained in this work were quite noisy at the wavelengths where haemoglobin absorption is the greatest. This is probably due to the fact that the probe was occasionally inadvertently placed over a blood vessel feeding the tumour. This source of error can be easily avoided in the future by observing the locations of feeder vessels on the tumour surface (visible through the thin skin of nude mice). Placing the fibre probe so as to avoid placement directly over a feeder vessel will reduce interference from haemoglobin and will provide a more reliable measurement of the tumour tissue itself. Another possible source of experimental error may be variations in the skin thickness over different tumour sites. It is also important to hold the probe properly over the site being measured. Significant deviations (30°) from normal incidence of the probe to the skin surface can also cause anomalous readings.

For absorption bands that do not overlap with haemoglobin, a greater sensitivity to the small changes in absorption can be achieved by using larger fibre separations and longer integration times. If the fibre separations are kept below 2.2 mm, this will not significantly increase the sensitivity to scattering.

4.2. Size of the tissue volume that is measured

A cross section of the tissue volume sampled by the photons is shown in figure 11. These results are from a Monte Carlo simulation performed with $\mu_a = 0.1$ cm^{-1}, $\mu_s = 100$ cm^{-1} and $g = 0.9$. The darker shaded regions indicate the locations where the collected photons underwent scattering events. Almost 50% of the scattering events occurred at a depth of less than 1 mm into the tissue and more than 75% occurred at a depth of less than 2 mm into the tissue.

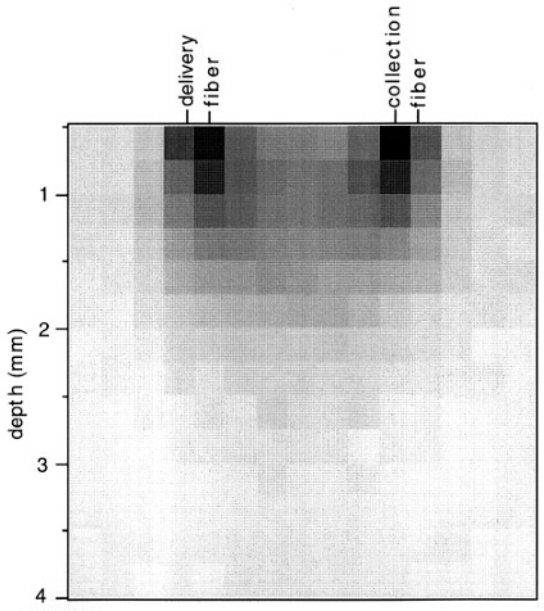

Figure 11. Image of the locations of scattering events of photons which are collected.

4.3. Measurement of drug in the tissue versus blood-borne drug

Any method that measures a tissue volume that is large compared with the size of a capillary vessel will not be able to easily distinguish between blood-borne and tissue-deposited agents. Standard invasive tissue-assay methods, such as biopsy combined with HPLC, have this trait since they incorporate any blood present in the tissue that is sampled. Interference from blood-borne drug with measurements of drug concentration in the tissue occurs only when drug levels in the blood significantly exceed those of the tissues, because blood accounts for only about 8% of body weight (Marieb 1992). Furthermore, it is only over a short period of time during and/or directly after the administration of the drug that the blood levels are significantly greater than those of the tissue. Due to the fact that drugs will accumulate in the tissues, and plasma drug concentrations will decrease over time due to drug distribution and excretion, plasma/tissue ratios will quickly favour tissue concentrations over plasma concentrations. For example, in one study where doxorubicin was administered, it was found that the doxorubicin concentration in the leukaemic cells was 175-fold higher than in the blood plasma at the end of a 45 min infusion period (Paul *et al* 1980). Thus, for the case of a measurement in a tissue with a high blood content, say 10%, 2 h after administration, when the ratio of the tissue-deposited to blood-borne agent might be, say, 3:1, the blood will contribute only about 3% of the total signal.

Optical measurements can have a major advantage over biopsy methods for distinguishing blood-borne and tissue concentrations. The absorption spectrum of a chemotherapy drug can change when the drug becomes localized in the tissue and binds to nucleic acids. This is illustrated in our measurements of mitoxantrone, where the measured absorption spectrum of mitoxantrone in the peritoneal cavity is consistent with nucleic acid-bound mitoxantrone. Therefore, the spectral change can potentially be used to distinguish blood-borne and tissue concentrations.

In some cases there may be significant value in the complementary use of the optical method described here and microdialysis. Once the drug has cleared from the blood, a combination of microdialysis and the optical method could provide detailed information about the location of the drug in tissue. Microdialysis will detect the drug only in the extracellular fluid, whereas the optical method will also be sensitive to drug residing in the cells. Therefore, it would be possible to track the diffusion/transport of the drug from the extracellular fluid into the cells.

5. Summary and conclusions

In previous work using tissue phantoms we demonstrated, that for the appropriate source–detector separations, the sensitivity of the pathlength travelled by the collected photons, L, on scattering is greatly reduced. Here we have extended the tissue phantom studies to an *in vivo* animal model.

The *in vivo* system is more complicated than the previous *in vitro* models which were studied. In order to address some of the issues regarding measurement and analysis of data from the *in vivo* system, additional measurements were made of tissue phantoms under different, yet still well-controlled, conditions. The issues addressed were the effect of changing the scattering parameters between measurements and the effect of strong intrinsic absorptions on L. A change in scattering properties during the time course of the measurements will not change L (in the geometry used in this work). However, a change in scattering properties can alter the amount of light that is collected. It was found that the simple addition of a baseline term in the analysis could be used to deal with this complication. Secondly, the issue of a change in pathlength due to the presence of an absorber was addressed. The dependence of pathlength on absorption was parametrized based on Monte Carlo simulations, and the values of the constants in the parametrization were determined from experimental measurements. Using these results, we were able to measure *in vivo* concentrations of two chemotherapy drugs in mice.

The results of the *in vivo* measurements are the site-specific time-histories of concentrations of mitoxantrone and doxorubicin (adriamycin) in nude mice. The site-specific measurements of mitoxantrone concentrations indicate that there may be significant variability in the uptake of this drug in different tumours. The time dependence of the measurements demonstrates that mitoxantrone continues to accumulate in the tumours over a period of at least 4 h. This is consistent with the known pharmacokinetics of mitoxantrone. The penetration of mitoxantrone into tissues is slow (Los *et al* 1989, Los and McVie 1990), and the redistribution back into blood plasma and clearance from the body are also slow processes (Batra *et al* 1986). Therefore mitoxantrone can be expected to accumulate in tissues slowly over time. Finally, the wavelength dependence of the optical spectra indicates that the measured mitoxantrone was bound to DNA. All of this is valuable information for the study of pharmacokinetics of a drug.

The results of optical measurements of doxorubicin at the time of sacrifice were compared with the absolute concentration as measured by HPLC analysis. A linear correlation was found, but the optical results were lower than the HPLC results by about 35%. The reasons for this discrepancy are at the moment unclear, but could be related to inaccuracies of the spectral shape and magnitude of the doxorubicin spectrum used in fitting the data or to inaccuracies in the coefficients of equation (3). In conclusion, we have demonstrated that elastic-scattering spectroscopy has the potential to provide quantitative, *in vivo*, site-specific measurements of drug concentrations.

Acknowledgments

This work was support by a Laboratory Directed Research and Development grant from Los Alamos National Lab. The authors gratefully acknowledge the work of Tina Giovanielli in measuring the haemoglobin spectra, of Jim Boyer in development of the software used in making some of these measurements and of Denis Heath in measuring the doxorubicin concentrations in tissues using HPLC.

References

Arcamone F M 1998 From the pigments of the actinomyecetes to third generation anthracyclines *Biochemie* **80** 201–6

Batra V K, Morrison J A, Woodward D L, Siverd N S and Yacobi A 1986 Pharmacokinetics of mitoxantrone in man and laboratory animals *Drug Metabol. Rev.* **17** 311–29

Bhatta N, Anderson R R, Flotte T, Schiff I, Hasan T and Nishioka N S 1992 Endometrial ablation by means of photodynamic therapy with photofrin II *Am. J. Obst. Gynecol.* **167** 1856–63

Blochl-daum B, Muller M, Meisinger V, Eichler H G, Fassolt A and Pehamberger H 1996 Measurement of extracellular fluid carboplatin kinetics in melanoma metastases with microdialysis *Br. J. Cancer* **73** 920–4

Braichotte D, Savary J-F, Monnier P, Wagnieres G and van den Bergh H 1996 Optimizing light dosimetry in photodynamic therapy of early stage carcinomas of the esophagus using fluorescence spectroscopy *Lasers Med. Sci.* **19** 340–6

Chang S C and Bown S G 1997 Photodynamic therapy: applications in bladder cancer and other malignancies *J. Formosan Med. Assoc.* **96** 853–63

Cheong W-F, Prahl S A and Welch A J 1990 A review of the optical properties of biological tissues *IEEE J. Quantum Electron.* **26** 2166–85

Choi Y S, Lee H J, Kwon J W, Kim W B, Yang J and Lee M G 1998 Pharmokinetic changes of M1, M2, M3 and M4 after intervenous administration of a new anthrocycline, DA-125, to rats pretreated with phenobarbital, 3-methylcholanthrene, chloramphenol or SKF-525A *Biopharmaceut. Drug Dispos.* **19** 78–89

Davies M I and Lunte C E 1995 Microdialysis sampling for hepatic-metabolism studies: impact of microdialysis probe design and implantation technique on liver tissue *Drug Metabol. Dispos.* **23** 1072–9

Di Marco A, Gaetani M and Scarpinato B 1969 Adriamycin (NSC-123, 127): a new antibiotic with antitumour activity *Cancer Chemother. Rep.* **55** 33–7

Donelli M G, Zucchetti M and Dincalci M 1992 Do anticancer agents reach the tumour target in the human brain? *Cancer Chemother. and Pharmacol.* **30** 251–60

Dougherty T J, Gomer C J, Henderson B W, Jori G, Kessel D, Korbelik M, Moan J and Peng Q 1998 Photodynamic Therapy *J. Natl Cancer Inst.* **90** 889–905

Eichler G H and Muller M 1998 Drug distribution: the forgotten relative in clinical pharmacokinetics *Clin. Pharmacol.* **34** 95–9

Fantini S, Franceschini M A, Fishkin J B, Barbieri B and Gratton E 1994 Quantitative determination of the absorption spectra of chromophores in strongly scattering media: a light-emitting-diode based technique *Appl. Opt.* **22** 5204–13

Farrell T J and Patterson M S 1992 A diffusion theory model of spatially resolved steady-state diffuse reflectance for the non-invasive determination of tissue optical properties *in vivo Med. Phys.* **19** 879–88

Fehr M K, Wyss P, Tromberg B J, Krasieva T, Disaia P J, Lin F and Tadir Y 1996 Selective photosensitizer localization in the human endometrium after intrauterine application of 5-aminoleuvelinic acid *Am. J. Obstet. Gynecol.* **175** 1253–9

Feofanov A, Sharonov S, Kudelina, Fluery F and Nabiev I 1997 Localization and molecular interactions of mitoxantrone within living K562 cells as probed by confocal spectral imaging analysis *Biophys. J.* **73** 3317–27

Ge Z, Schomaker K T and Nishioka N S 1998 Identification of colonic dysplasia and neoplasia by diffuse reflectance spectroscopy and pattern recognition *Appl. Spectrosc.* **52** 833–9

Henyey L G and Greenstein J L 1941 Diffuse radiation in the galaxy *Astrophys. J.* **93** 70–83

Humpel C, Chadi G, Lippoldt A, Ganten D, Fuxe K and Olson L 1994 Increase of basic fibroblast growth factor, messenger RNA and protein following implantation of a microdialysis probe into rat hippocampus *Exp. Brain Res.* **98** 229–37

Humpel C, Ebendal T and Olson L 1996 Microdialysis: a way to study *in-vivo* release of neurotrophic bioactivity: a critical summary *J. Mol. Med.* **74** 523–6

Jacques S L, Saidi I, Ladner A and Oelberg D 1997 Developing an optical fiber reflectance spectrometer to monitor bilirubinemia in neonates *Proc. SPIE* **2975** 115–24

Jacques S L and Wang L 1995 Monte Carlo modeling of light transport in tissues *Optical-Thermal Response of Laser Irradiated Tissue* ed A J Welch and van J C Gemert (New York: Plenum) pp 73–100

Kerr D J and Los G 1993 Pharmacokinetic principles of locoregional chemotherapy *Cancer Surv.* **17** 105–22

Layton M E, Pazdernik T L and Samson F E 1997 Cerebral penetration injury leads to H202 generation in microdialysis samples *Neurosci. Lett.* **236** 63–6

Levy J G 1994 Photosensitizers in photodynamic therapy *Semin. Oncol.* **21** 4–10

Lin S-P, Wang L H, Jacques S L and Titel F K 1997 Measurement of tissue optical-properties by the use of oblique incidence optical-fibre reflectometry *Appl. Opt.* **36** 136–43

Los G and McVie J G 1990 Experimental and clinical status of intraperitoneal chemotherapy *Eur. J. Cancer* **26** 755–62

Los G, Ruevekamp M, Bosnie N, De Graaf P W and McVie J G 1989 Intraperitoneal tumour growth and chemotherapy in a rat model *Eur. J. Cancer Clin. Oncol.* **25** 1857–66

Marieb E N 1992 *Human Anatomy and Physiology* (New York: Benjamin-Cummings) p 579

Mewes K, Blanz J, Ehninger G, Gebhardt R and Zeller K-P 1993 Cytochrome P-450-induced cytotoxicity of mitoxantrone by formation of electrophilic intermediates *Cancer Res.* **53** 5135–42

Mourant J R, Bigio I J and Boyer J 1995 Spectroscopic diagnosis of bladder cancer with elastic light scattering *Lasers Surgery Med.* **16** 350–7

Mourant J R, Bigio I J, Boyer J, Johnson T, Lacey J, Bohorfoush G and Mellow M 1996a Elastic scattering spectroscopy as a diagnostic tool for differentiating pathologies in the gastrointestinal tract: preliminary testing *J. Biomed. Opt.* **1** 192–9

Mourant J R, Bigio I J, Jack D A, Johnson T M and Miller H D 1997a Measuring absorption coefficients in small volumes of highly scattering media: source–detector separations for which pathlengths do not depend on scattering properties *Appl. Opt.* **36** 5655–61

Mourant J R, Boyer J, Hielscher A H and Bigio I J 1996b Influence of the scattering phase function on light transport measurements in turbid media performed with small source–detector separations *Opt. Lett.* **21** 546–8

Mourant J R, Fuselier T, Boyer J, Johnson T and Bigio I J 1997b Predictions and measurements of scattering and absorption over broad wavelength ranges in tissue phantoms *Appl. Opt.* **36** 949–57

Nichols M G, Hull E L and Foster T H 1997 Design and testing of a white-light, steady-state diffuse reflectance spectrometer for determination of optical properties of highly scattering systems *Appl. Opt.* **36** 93–104

Patterson M S, Moulton J D, Wilson B C and Chance B 1990 Applications of time-resolved scattering measurements to photodynamic therapy *Proc. SPIE* **1203** 62–75

Paul C, Baurain R, Gahrton G and Peterson C 1980 Determination of daunorubicin and its main metabolites in plasma, urine and leukaemic cells in patients with acute myeloblastic leukaemia *Cancer Lett.* **9** 263–9

Perelman L T *et al* 1998 Observation of periodic fine structure in reflectance from biological tissue: a new technique for measuring nuclear size distribution *Phys. Rev. Lett.* **80** 627–30

Porumb H 1978 The solution spectroscopy of drugs and the drug-nucleic acid interaction *Prog. Biophys. Mol. Biol.* **34** 175–95

Ratkay L G, Chowdhary R K, Iamaroon A, Richter A M, Neyndorff H C, Keystone E C, Waterfield J D and Levt J G 1998 Amelioration of antigen-induced arthritis in rabbits by induction of apoptosis of inflammatory cells with local application of transdermal photodynamic therapy *Arthritis Rheumatism* **41** 525–34

Rhodes L E, Tsoukas M M, Anderson R R and Kollias N 1997 Iontophoretic delivery of ALA provides a quantitative model for ALA pharmacokinetics and PPIX phototoxicity in human skin *J. Invest. Dermatol.* **108** 87–91

Rossomondo E F and Kehr J 1998 Microdialysis: an *in vivo* method for analysis of body fluids *Methods Biochem. Anal.* **38** 115–36

Schmitt J M and Kumar G 1997 Optimal probe geometry for near-infrared spectroscopy of biological tissue *Appl. Opt.* **36** 2286–93

Schuitmaker J J, Baas P, van Leengoed H L L M, van der Muelen F M, Star W M and van Zandwijk N 1996 Photodynamic therapy: a promising new modality for the treatment of cancer *J. Photochem. and Photobiol.* **34** 3–12

Star W M 1997 Light dosimetry *in vivo Phys. Med. Biol.* **42** 763–87

Stevens C L, Taylor K G, Munk M E, Marshall W S, Noll K, Shah G D, Shah L G and Uzu K J 1965 Chemistry and structure of Mitomycin C *Med. Chem.* **8** 1–10

Wang L H, Jacques S L and Weng L 1995 *Comput. Methods Programs Biomed.* **47** 131–46

Webb J S *et al* 1962 The structures of mitomycins A, B and C and porfiromycin—part I *J. Am. Chem. Soc.* **84** 3185–7

Weersink R A, Hayward J E, Diamond K R and Patterson M S 1997 Accuracy of non-invasive *in vivo* measurements of photosensitizer uptake based on a diffusion model of reflectance spectroscopy *J. Photochem. Photobiol.* **66** 326–35

Wilson B C 1995 Measurement of tissue optical properties: methods and theories *Optical-Thermal Response of Laser-Irradiated Tissue* ed A J Welch and M J C van Gemert (New York: Plenum) pp 233–74

Zijlstra W G 1991 Absorption spectra of human fetal and adult oxyhaemoglobin, de-oxyhaemoglobin, carboxyhaemoglobin, and methaemoglobin *Clin. Chem.* **37** 1633–8